INTERNATIONAL JOURNAL OF PLANT, ANIMAL AND ENVIRONMENTAL SCIENCES
IJPAES
VOLUME-2, ISSUE-4, OCT-DEC-2012 ISSN 2231-4490

Coden : IJPAES www.ijpaes.com

Received: 19th Sept-2012 *Revised: 25th Sept-2012* *Accepted: 30th Sept-2012*

Research article

HOMOLOGY MODELING AND DOCKING STUDIES OF BCL2L10-HUMAN INVOLVED IN CANCER

S.Murali Mohan[1]., Mohammad HekmatAfshar[2]., Mohammad Munawar[3]., D.Jayasimha Rayalu[4*]

[1]Department of Zoology., S.S.B.N Degree and P.G College, Anantapur, Andhra Pradesh. INDIA.
[2]Department of Microbiology., Islamic Azad University of Jahrom, IRAN.
[3]Department of Biotechnology., JNTUACEP. INDIA
[4]Department of Biotechnology., DR.Rayalu's Biotech pvt.LTD. Hyderabad.

ABSTRACT: Homology modeling and flexible docking of Bcl2L10 has been studied in *silico* approach. Blast result was found to have similarity with Bcl2L10 of 48% identity with 2KUA. Active site of Bcl2L10 was identified by CASTP. Large potential drugs were designed for identifying molecules that can likely bind to protein target of interest. The different drug derivatives designed were used for docking with the generated structure, among the 100 derivatives designed, fifth derivative showed highest docking result. The drug derivatives were docked to the protein by hydrogen bonding interactions and these interactions play an important role in the binding studies. Our investigations may be helpful for further studies.

Key words: BCL2, Cancer, homology modeling, drug designing, docking studies

INTRODUCTION

In order to propagate, cells need to execute a cell division cycle, or cell cycle. The notion of the cell cycle refers to the ordered sequence of events that controls and coordinates the accurate duplication and segregation of the genetic information of a cell that guarantees the genetic stability between one cell and its progeny. The cell cycle is composed of four phases the G1 and G2 gap-phases, the Synthetic S-phase, and the Mitotic Mphase [3, 6]. In a human under normal condition on an average a cell can undergo division for 52 times and after that it may undergo programmed cell death [12]. This process of cell suicide or programmed cell death is called as Apoptosis which may be occurred in physiological and diseased conditions [4]. It is estimated that about 50 to 70 billion cells die each day due to apoptosis in the average human adult. Averagely for a child between the ages of 8 and 14, approximately 20 billion to 30 billion cells die in a day [8]. Disruption of the regulation of apoptosis may result in various diseases, including cancer associated with the inhibition of apoptosis and neurodegenerative disorders associated with the enhancement of apoptosis. Cancer is a disease that begins in the cells of the body which is characterized by uncontrolled, uncoordinated and undesirable cell division. If a cell accumulates critical mutations in five or six of the proto-oncogenes, tumour suppressor genes and DNA repair genes are likely to result in a fully malignant cell, capable of forming a tumour. Apoptosis is a multi-path way mechanism which involves the action of many proteins. Among them BCL2 family plays a very important role in promoting or in inhibiting apoptosis**.** BCL2 gene (otherwise B-cell lymphoma 2 gene, bcl-2) was first discovered in follicular B-cell lymphoma as a gene which is linked to the immunoglobulin heavy chain locus at the breakpoints of t(14;18) translocation; the result of this translocation is the enhanced BCL2 protein transcription. In normal cells this gene is located on chromosome segment 18q21.3. BCL2 protein was found to inhibit cell death [11]. Bcl-2, the first anti-cell death gene belongs to BCL2 family of proteins is the hallmark of apoptosis regulation. The disturbance of apoptosis molecular signaling pathways is involved in carcinogenesis. Mammalian BCL2 protein family consists of at least 30 related proteins, characterized by the presence of up to four relatively short sequence motifs (less than 20 amino acid residues in length) termed BCL2 homology (BH) domains [2,1]. BCL2 family is divided into three different subclasses based on structural and functional features [8]. The prosurvival or anti apoptotic subfamily includes BCL2, BCL-XL, BCL-W, and MCL-1 proteins, which possess all four conserved BH domains, designated BH1-4, and a hydrophobic C terminal part. BH1-BH3 domains form a hydrophobic groove and the N-terminal BH4 domain stabilizes this structure [Robert Eskes et al 2000]. BH4 domain is usually absent in apoptotic proteins and therefore is a key factor for the anti apoptotic activity.

BCL2 is permanently found in membranes, whereas BCL-XL and BCL-W are linked to the membrane after a cytotoxic signal [Reed et al 2004]. BCL2 (and its anti apoptotic orthologues) seems to inhibit apoptosis by the preservation of mitochondrial membrane integrity as its hydrophobic carboxyl-terminal domain is linked to the outer membrane. BCL2 prevents BAX/BAK oligomerization, which would otherwise lead to the release of several apoptogenic molecules from the mitochondrion. It is also known that BCL2 binds to and inactivates BAX and other pro-apoptotic proteins, thereby inhibiting apoptosis [7]. BCL2 might also regulate the activation of several initiator caspases like caspase-2 that act upstream or independently of cytochrome c release from mitochondria. Moreover, BCL2 directly blocks cytochrome c release and therefore prevents APAF-1 and caspase-9 activation [9].

MATERIALS AND METHODS

3D model building

Homology modeling, also known as comparative modeling refers to constructing an atomic-resolution model of the "*target*" protein from its amino acid sequence and an experimental three-dimensional structure of a related homologous protein (the "*template*"). Homology modeling relies on the identification of one or more known protein structures likely to resemble the structure of the query sequence, and on the production of an alignment that maps residues in the query sequence to residues in the template sequence. The sequence alignment and template structure are then used to produce a structural model of the target. Because protein structures are more conserved than DNA sequences, detectable levels of sequence similarity usually imply significant structural similarity. Suppose you want to know the 3D structure of a target protein that has not been solved empirically by X-ray crystallography or NMR. You have only the sequence. If an empirically determined 3D structure is available for a sufficiently similar protein (50% or better sequence identity would be good), you can use software that arranges the backbone of your sequence identically to this template. This is called "homology modeling". It is, at best, moderately accurate for the positions of alpha carbons in the 3D structure, in regions where the sequence identity is high. It is inaccurate for the details of side chain positions, and for inserted loops with no matching sequence in the solved structure. The optimization procedure is a variable target function method that applies the conjugate gradients algorithm to positions of all non-hydrogen atoms. The query sequence from Homo sapiens was submitted to domain fishing server prediction. The predicted domain was searched to find out the related protein structure to be used as a template by the BLAST (Basic Local Alignment Search Tool) program against PDB (Protein Databank). Sequence that showed maximum identity with high score and less e-value was aligned and Bile salt export pump was used as a reference structure to build a 3D model for. The sequence of Bile salt export pump was obtained from UNIPROT. The co-ordinates for the structurally conserved regions (SCRs) for BCL2L10 were assigned from the template using multiple sequence alignment, based on the Needleman-Wunsch algorithm. The structure having the least modeller objective function, obtained from the modeller was improved by molecular dynamics and equilibration methods using NAMD 2.5 software using CHARMM27 force field for lipids and proteins along with the TIP3P model for water. The energy of the structure was minimized with 1, 00, 00 steps. A cutoff of 12 Å (switching function starting at 10 Å) for van der Waals interactions was assumed. No periodic boundary conditions were included in this study. An integration time step of 2 fs was used, permitting a multiple time-stepping algorithm to be employed in which interactions involving covalent bonds were computed every time step, short-range non bonded interactions were computed every two time steps and long-range electrostatic forces were computed every four time steps. The pair list of the non bonded interaction was recalculated every ten time steps with a pair list distance of 13.5 Å. The short-range non bonded interactions were defined as van der Waals and electrostatics interactions between particles within 12 Å. A smoothing function was employed for the van der Waals interactions at a distance of 10 Å. CHARMM27 [force-field parameters were used in all simulations in this study. The equilibrated system was simulated for 1 ps with a 500 kcal/mol/Å2 restraint on the protein backbone under 1 atm constant pressure and 310 K constant temperature (NPT) and the Langevin damping coefficient was set to 5 ps unless otherwise stated. Finally, the structure having the least energy with low RMSD (Root Mean Square Deviation) was used for further studies. In this step, the quality of the initial model was improved. The final structure obtained was analyzed by Ramachandran's map using PROCHECK (Programs to check the Stereo chemical Quality of Protein Structures) and environment profile using ERRAT graph (Structure Evaluation server). This model was used for the identification of active site and for docking of the substrate with the enzyme.

Active site Identification

Active site of BCL2L10 was identified using CASTp server. A new program, CASTp, for automatically locating and measuring protein pockets and cavities, is based on precise computational geometry methods, including alpha shape and discrete flow theory. CASTp identifies and measures pockets and pocket mouth openings, as well as cavities. The program specifies the atoms lining pockets, pocket openings, and buried cavities; the volume and area of pockets and cavities; and the area and circumference of mouth openings.

Docking method

Docking was carried out using GOLD (Genetic Optimization of Ligand Docking) software which is based on genetic algorithm (GA). This method allows as partial flexibility of protein and full flexibility of ligand. The compounds are docked to the active site of the Bcl2L10. The interaction of these compounds with the active site residues are thoroughly studied using molecular mechanics calculations. The parameters used for GA were population size (100), selection pressure (1.1), number of operations (10,000), number of island (1) and niche size (2). Operator parameters for crossover, mutation and migration were set to 100, 100 and 10 respectively. Default cutoff values of 3.0 A° (dH-X) for hydrogen bonds and 6.0 A° for vanderwaals were employed. During docking, the default algorithm speed was selected and the ligand binding site in the alpha glucosidase was defined within a 10 A° radius with the centroid as CE atom of ALA410. The number of poses for each inhibitor was set 100, and early termination was allowed if the top three bound conformations of a ligand were within 1.5A° RMSD. After docking, the individual binding poses of each ligand were observed and their interactions with the protein were studied. The best and most energetically favorable conformation of each ligand was selected.

Gold Score fitness function:

Gold Score performs a force field based scoring function and is made up of four components: 1. Protein-ligand hydrogen bond energy (external H-bond); 2. Protein-ligand vander Waals energy (external vdw); 3. Ligand internal vander Waals energy (internal vdw); 4. Ligand intramolecular hydrogen bond energy (internal- H- bond). The external vdw score is multiplied by a factor of 1.375 when the total fitness score is computed. This is an empirical correction to encourage protein-ligand hydrophobic contact. The fitness function has been optimized for the prediction of ligand binding positions.

GoldScore = S (hb_ext) + S (vdw_ext) + S (hb_int) + S (vdw_int)

Where S (hb_ext) is the protein-ligand hydrogen bond score, S (vdw_ext) is the protein-ligand van der Waals score, S (hb_int) is the score from intramolecular hydrogen bond in the ligand and S (vdw_int) is the score from intramolecular strain in the ligand.

RESULTS AND DISCUSSION

Homology modeling of BCL2L10

A high level of sequence identity should guarantee more accurate alignment between the target sequence and template structure. In the results of BLAST search against PDB, only the 2KUA which has a high level of sequence identity with the BCL2L10 domain (48%). Structurally conserved regions (SCRs) for the model and the template were determined by sequence alignment and the SCRs were determined as shown by Fig.1.

In the following study, we have chosen 2KUA as a reference structure for modeling BCL2L10 domain. Coordinates from the reference protein (2KUA) to the SCRs, structurally variable regions (SVRs), N-termini and C-termini were assigned to the target sequence based on the satisfaction of spatial restraints. In the modeller we will get a 20 PDB out of which we select a least energy. The energy unit will be in kilo joule. All side chains of the model protein were set by rotamers. The final stable structure of the BCL2L10 protein obtained is shown in Figure 2. By the help of SPDBV it is evident that BCL2L10 domain has 7 helices.

The final structure was further checked by verify3D graph and the results have been shown in Figure 3: The overall scores indicates acceptable protein environment.

Validation of BCL2L10 Domain

After the refinement process, validation of the model was carried out using Ramachandran plot calculations computed with the PROCHECK program (Figure 4). The distributions of the Ramachandran plots of non-glycine, non-proline residues are summarized in Table 1. The RMSD (Root Mean Square deviation) deviation for covalent bonds and covalent angles relative to the standard dictionary of BCL2L10 was -1.26 and -0.25 Å. Altogether 98.8 % of the residues of BCL2L10 was in favored and allowed regions. The overall PROCHECK G-factor of BCL2L10 was – 2.32 and verify3D environment profile was good.

```
Sequence type explicitly set to Protein
Sequence format is Pearson
Sequence 1: template     165 aa
Sequence 2: query        194 aa
Start of Pairwise alignments
Aligning...


Sequences (1:2) Aligned. Score: 44.8485
Guide tree file created:   [clustalw.dnd]

There are 1 groups
Start of Multiple Alignment

Aligning...
Group 1: Sequences:   2      Score:1284
Alignment Score 481

CLUSTAL-Alignment file created  [clustalw.aln]
```

```
clustalw.aln

CLUSTAL 2.1 multiple sequence alignment


template        MADSQDPLHERTRRLLSDYIFFCAREPDTPEPPPTSVEAALLRSVTRQIQQEHQEFFSSF
query           ---MADPLRERTELLLADYLGYCAREPGTPEPAPSTPEAAVLRSAAARLRQIHRSFFSAY
                     ***:***. **:**: :*****.****.*:: ***:***.: :::* *:.***::

template        CESRGNRLELVKQMADKLLSKDQDFSWSQLVMLLAFAGTLMNQGPYMAVKQKRD------
query           LGYPGNRFELVALMADSVLSDSPGPTWGRVVTLVTFAGTLLERGPLVTARWKKWGFQPRL
                    ***:***  ***.:**.. . :*.::* *::*****:::** ::.: *:

template        LGNRVIVTRDCCLIVNFLYNLLMGRRHRARLEALGGWDGFCRFFKNPLPLG---------
query           KEQEGDVARDCQRLVALLSSRLMG-QHRAWLQAQGGWDGFCHFFRTPFPLAFWRKQLVQA
                  :.  *:***  :* :* . *** :*** *:* *******:**:.*:**.

template        ------------------
query           FLSCLLTTAFIYLWTRLL
```

Fig 1: CLUSTAL 2.0.11 multiple sequence alignment

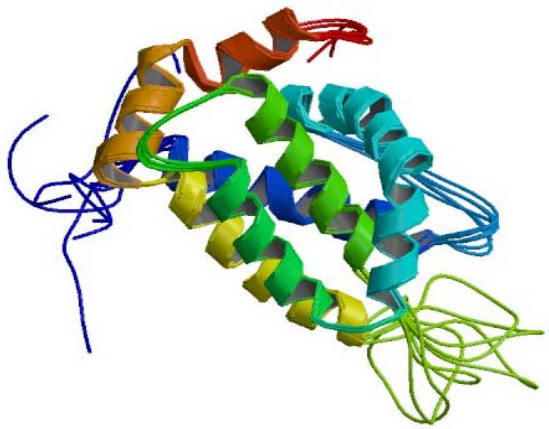

Fig 2: Three dimensional structure of BCL2L10

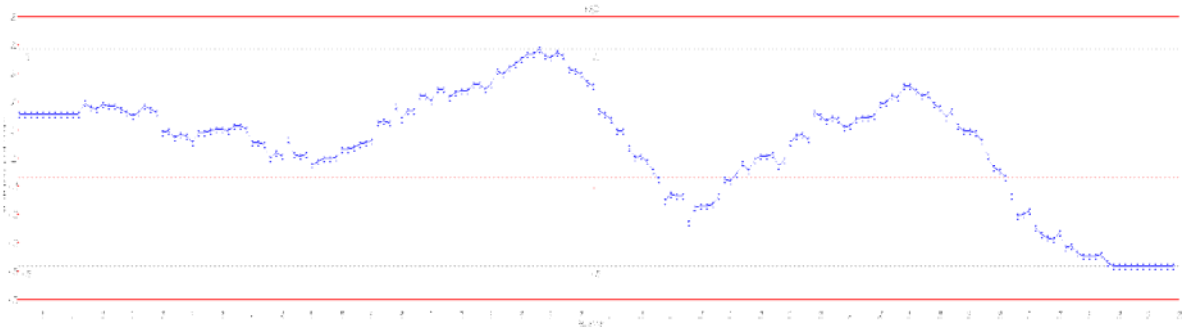

Fig 3: Verify 3D graph of BCL2L10

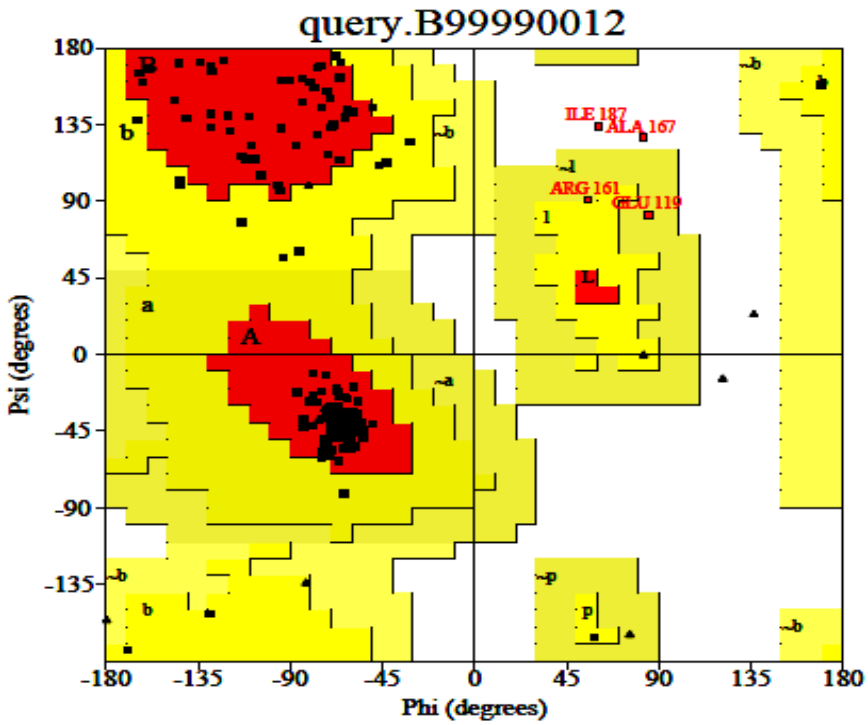

Fig 4 : Ramachandran plot

Superimposition of 2KUA with BCL2L10 domain

The structural superimposition of 2KUA template and BCL2L10 is shown in Figure V. The weighted root mean square deviation of trace between the template and final refined models 0.90A^{o}. This final refined model was used for the identification of active site and for docking of the substrate with the domain BCL2L10.

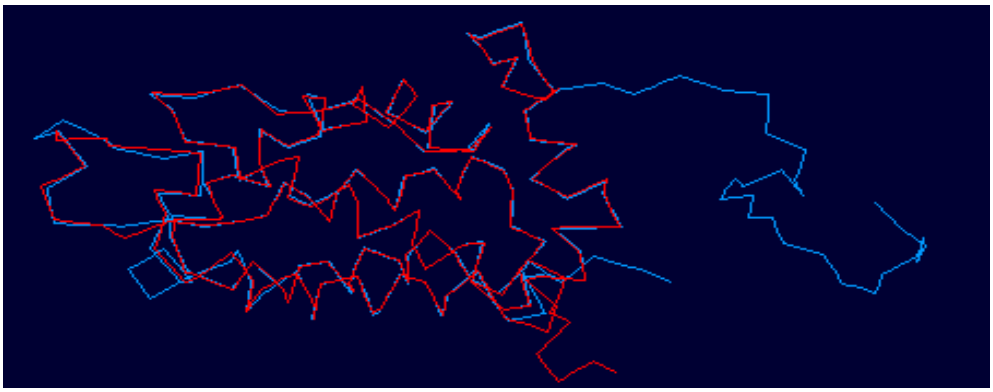

Fig 5: Superimposition of BCL2L10 (Blue colour) with Template 2KUA (Red colour)

Active site Identification of BCL2L10 domain

After the final model was built, the possible binding sites of BCL2L10 was searched based on the structural comparison of template and the model build and also with CASTP server and was shown in Figure VI. Since, BCL2L10 from Human and the 2KUA are well conserved in both sequence and structure; their biological function should be identical. It was found that secondary structures are highly conserved and the residues, GLY6, ILE8, ILE9, ASN10, GLY14, LEU18, SER20, GLN22, CYS28, THR32, HIS151, PRO180, GLY250, PRO309, VAL321, PHE321.

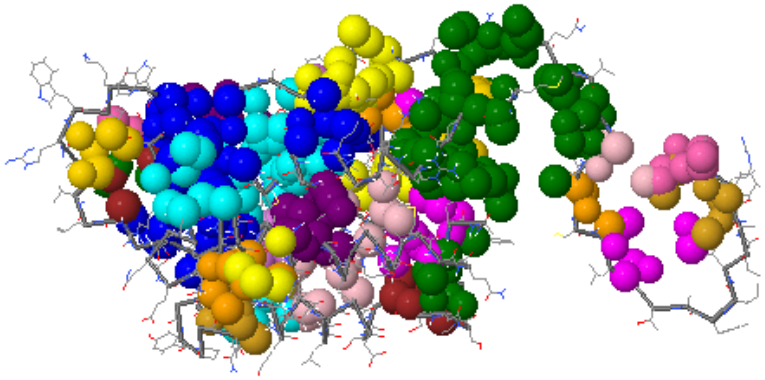

Fig 6: Active site of protein

Docking of inhibitors with the active site of BCL2L10

Docking of the inhibitors with BCL2L10 was performed using GOLD 3.0.1, which is based on genetic algorithimn (Figure 7). This program generates an ensemble of different rigid body orientations (poses) for each compound conformer within the binding pocket and then passes each molecule against a negative image of the binding site. Poses clashing with this 'bump map' are eliminated. Poses surviving the bump test are then scored and ranked with a Gaussian shape function. We defined the binding pocket using the ligand-free protein structure and a box enclosing the binding site. This box was defined by extending the size of a cocrystalized ligand by 4A. This dimension was considered here appropriate to allow, for instance, compounds larger than the cocrystallized ones to fit into the binding site. One unique pose for each of the best-scored compounds was saved for the subsequent steps. The compounds used for docking was converted in 3D with SILVER. To this set, the substrate corresponding to the modeled protein were added. Docking of best inhibitor with the active site of protein showed the activity of the molecule on protein function (Fig 8).

Chemical structure (inhibitor) of drugs that designed for using on docking in the study

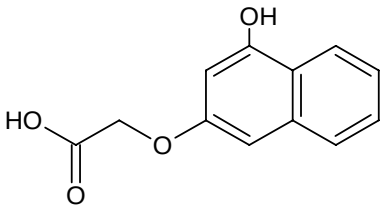

[(4-hydroxy-2-naphthyl)oxy]acetic acid

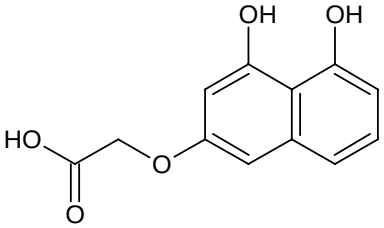

[(4,5-dihydroxy-2-naphthyl)oxy]acetic acid

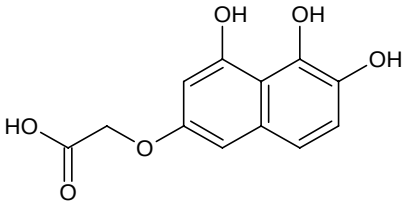

[(4,5,6-trihydroxy-2-naphthyl)oxy]acetic acid

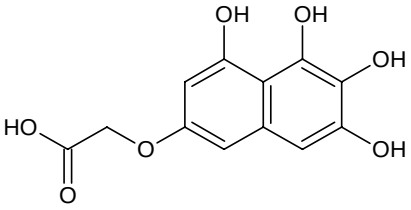

[(4,5,6,7-tetrahydroxy-2-naphthyl)oxy]acetic acid

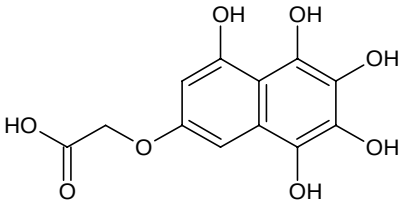

[(4,5,6,7,8-pentahydroxy-2-naphthyl)oxy]acetic acid

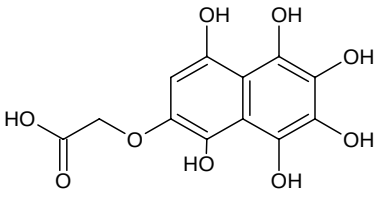

[(1,4,5,6,7,8-hexahydroxy-2-naphthyl)oxy]acetic acid

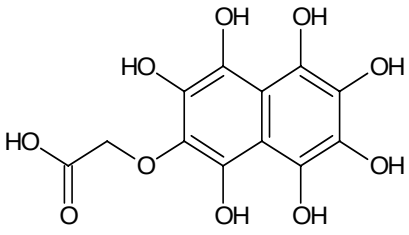

[(1,3,4,5,6,7,8-heptahydroxy-2-naphthyl)oxy]acetic acid

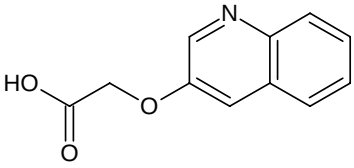

(quinolin-3-yloxy)acetic acid

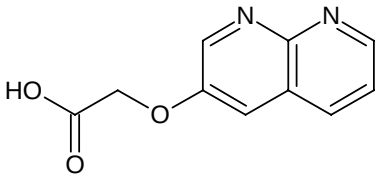

(1,8-naphthyridin-3-yloxy)acetic acid

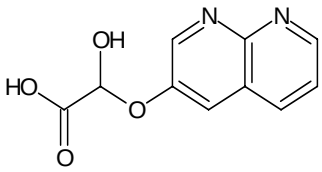

hydroxy(1,8-naphthyridin-3-yloxy)acetic acid

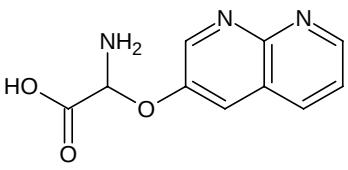

amino(1,8-naphthyridin-3-yloxy)acetic acid

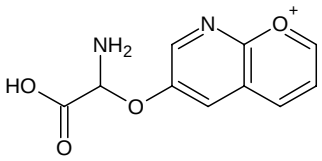

6-[amino(carboxy)methoxy]pyrano[2,3-*b*]pyridin-1-ium

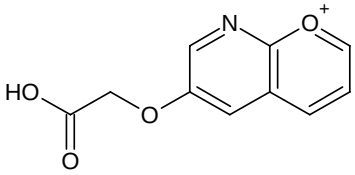

6-(carboxymethoxy)pyrano[2,3-*b*]pyridin-1-ium

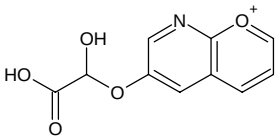

6-[carboxy(hydroxy)methoxy]pyrano[2,3-*b*]pyridin-1-ium

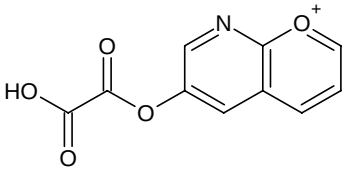

6-[(carboxycarbonyl)oxy]pyrano[2,3-*b*]pyridin-1-ium

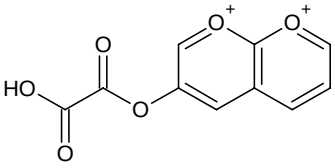

3-[(carboxycarbonyl)oxy]pyrano[2,3-*b*]pyrandiium

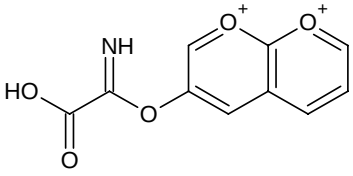

3-[carboxy(imino)methoxy]pyrano[2,3-*b*]pyrandiium

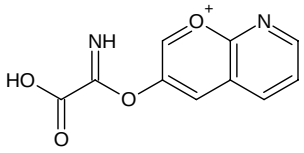

3-[carboxy(imino)methoxy]pyrano[2,3-*b*]pyridin-1-ium

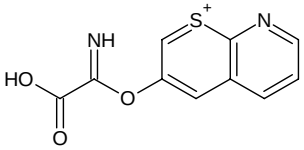

3-[carboxy(imino)methoxy]thiopyrano[2,3-*b*]pyridin-1-ium

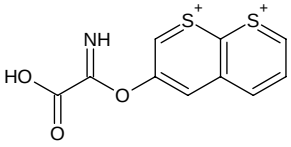

3-[carboxy(imino)methoxy]thiopyrano[2,3-*b*]thiopyrandiium

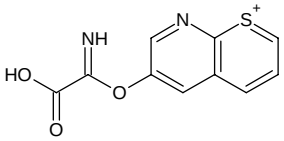

6-[carboxy(imino)methoxy]thiopyrano[2,3-*b*]pyridin-1-ium

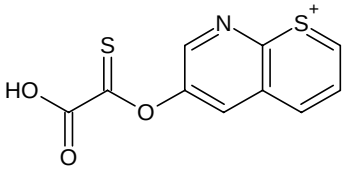

6-[(carboxycarbonothioyl)oxy]thiopyrano[2,3-*b*]pyridin-1-ium

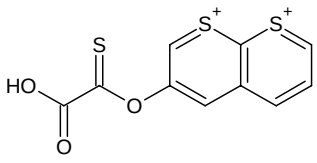

3-[(carboxycarbonothioyl)oxy]thiopyrano[2,3-*b*]thiopyrandiium

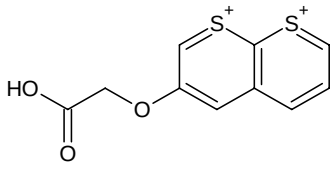

3-(carboxymethoxy)thiopyrano[2,3-*b*]thiopyrandiium

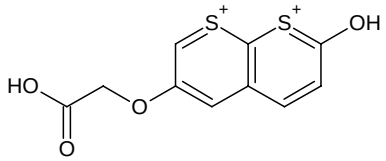

6-(carboxymethoxy)-2-hydroxythiopyrano[2,3-*b*]thiopyrandiium

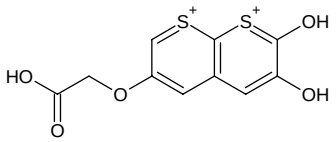

6-(carboxymethoxy)-2,3-dihydroxythiopyrano[2,3-*b*]thiopyrandiium

Fig 7: Different compounds were checked for the docking with protein Bcl2L10 as following:

Docking

Docking of the inhibitors with BCL2L10 was performed using GOLD 3.0.1, which is based on genetic algorithimn. This program generates an ensemble of different rigid body orientations (poses) for each compound conformer within the binding pocket and then passes each molecule against a negative image of the binding site. Poses clashing with this 'bump map' are eliminated. Poses surviving the bump test are then scored and ranked with a Gaussian shape function. We defined the binding pocket using the ligand-free protein structure and a box enclosing the binding site. This box was defined by extending the size of a cocrystalized ligand by 4 Å. This dimension was considered here appropriate to allow, for instance, compounds larger than the cocrystallized ones to fit into the binding site. One unique pose for each of the best-scored compounds was saved for the subsequent steps. The compounds used for docking was converted in 3D with SILVER. To this set, the substrate corresponding to the modeled protein were added. Docking of inhibitors with the active site of protein Bcl2L10.

Table 1: Individual for each ligand docked with protein in GOLD

Fitness	S(hb_ext)	S(vdw_ext)	S(hb_int)	S(int)	Ligand name
35.52	8.00	22.72	0.00	-3.72	soln_1_m1_1.mol2
38.50	12.67	20.18	0.00	-1.91	soln_10_m1_5.mol2
40.11	13.73	21.46	0.00	-3.14	soln_11_m1_4.mol2
34.37	6.00	21.79	0.00	-1.60	soln_12_m1_2.mol2
32.49	6.00	20.20	0.00	-1.28	soln_13_m1_1.mol2
35.12	6.04	23.07	0.00	-2.65	soln_14_m1_1.mol2
34.16	8.00	20.11	0.00	-1.49	soln_15_m1_4.mol2
31.05	6.00	21.43	0.00	-4.42	soln_16_m1_10.mol2
33.69	6.34	23.56	0.00	-5.04	soln_17_m1_3.mol2
31.69	5.99	22.52	0.00	-5.27	soln_18_m1_7.mol2'
32.32	7.65	19.20	0.00	1.72	soln_19_m1_6.mol2
34.46	15.77	17.40	0.00	-5.24	soln_2_m1_5.mol2
33.84	4.73	23.67	0.00	-3.44	soln_20_m1_2.mol2
35.31	8.86	22.26	0.00	-4.16	soln_21_m1_9.mol2
36.31	1.80	26.38	0.00	-1.76	soln_22_m1_1.mol2
36.31	4.56	25.21	0.00	-2.91	soln_23_m1_9.mol2
35.34	4.75	24.03	0.00	-2.44	soln_24_m1_3.mol2
37.17	5.31	25.58	0.00	-3.31	soln_25_m1_1.mol2
37.38	14.44	19.88	0.00	-4.39	soln_26_m1_1.mol2
33.56	13.20	19.41	0.00	-6.34	soln_3_m1_5.mol2
33.63	12.78	19.41	0.00	-5.84	soln_4_m1_7.mol2'
29.81	11.39	18.79	0.00	-7.41	soln_5_m1_4.mol2
33.94	14.15	20.65	0.00	-8.60	soln_6_m1_6.mol2
32.63	13.71	21.48	0.00	-10.61	soln_7_m1_1.mol2
33.42	7.53	20.01	0.00	-1.63	soln_8_m1_6.mol2
33.60	1.25	25.64	0.00	-2.91	soln_9_m1_2.mol2

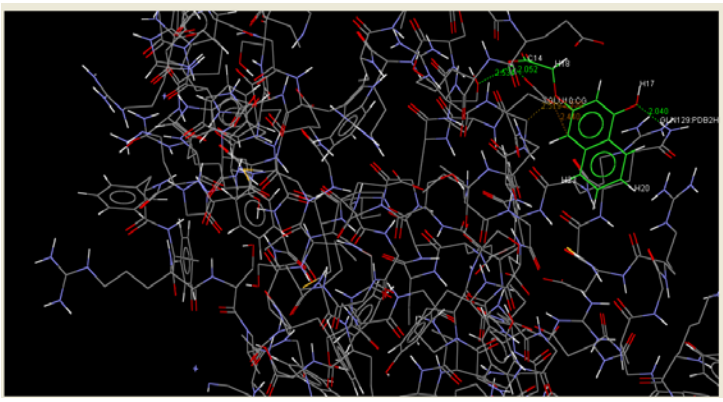

Figure 8: Docking of Bcl2L10 with drug on level 40.11

CONCLUSION

Despite the great interest of efforts for cancer treatment still remains the need to investigate more because no much effect of actively arresting this disease. In this work, we have constructed a 3D model of Bcl2L10, using the MODELLER software and obtained a refined model after energy minimization. The final refined model was further assessed by ERRAT and PROCHECK program, and the results show that this model is reliable. Only protein2KUA (chain A) has a high level of coverage (85%), total score (137) and identity (48%) of the reference protein with the Bcl2L10are 48%. Docking results indicate that conserved amino-acid residues Bcl2 mainly play an important role in maintaining a functional conformation and are directly involved in donor substrate binding. The interaction between the domain and the inhibitors proposed in this study are useful for understanding the potential mechanism of domain and the inhibitor binding.

As is well known, hydrogen bonds play important role for the structure and function of biological molecules. In this study it was found that,* [(3,4,5-trihydroxy-6-{[(3,4,5,6-tetrahydroxytetrahydro-2*H*-pyran-2-yl)oxy]methyl} tetrahydro-2*H*-pyran-2-yl)oxy]ethanethial,*{2-[2-oxo-2-(phosphinooxy)ethoxy]naphthalene-1,4-diyl} diphosphine,*{3-[2-oxo-2-(phosphinooxy)ethoxy]-1-naphthyl}phosphine,* 3,4, 5-trihydroxy-6-{[(3,4,5,6-tetrahydroxytetrahydro-2*H*-pyran2yl)oxy]methyl}tetrahydro-2*H*-pyran-2-yl imidoformate and *Amino(1,8-naphthyridin-3-yloxy) acetic acid are important for strong hydrogen bonding interaction with the inhibitors. Based on these findings, we have developed the hypothesis that the inhibition of Bcl2L10 is possible by some drugs.

REFFERENCES

[1] Boise, Lawrence H.Gonzalez-Garcia, Maribel Postema, Christina E.Ding, Liyun Lindsten, Tullia Turka, Laurence A.Mao, Xiaohong Nunez, Gabriel Thompson, Craig B. 1993 bcl-x, a bcl-2-related gene that functions as a dominant regulator of apoptotic cell death. Cell, Vol. 74, 597-606.

[2] Flora Tzifi, Christina Economopoulou, Dimitrios Gourgiotis, Alexandros Ardavanis, Sotirios Papageorgiou, and Andreas Scorilas 2012 The Role of BCL2 Family of Apoptosis Regulator Proteins in Acute and Chronic Leukemias. Advances in Hematology.

[3] Green, Douglas 2011. Means To An End. New York: Cold Spring Harbor Laboratory Press. ISBN 978-87969-888-1.

[4] J. C. Reed, 2006 "Proapoptoticmultidomain Bcl-2/Bax-family proteins: mechanisms, physiological roles, and therapeutic opportunities," Cell Death and Differentiation, vol. 13, no. 8, pp. 1378–1386.

[5] J. C. Reed, 2004 "Apoptosis mechanisms: implications for cancer drug discovery," Oncology, vol. 18, supplement 10, no. 13, pp. 11–20.

[6] Karam, Jose A. 2009. Apoptosis in Carcinogenesis and Chemotherapy. Netherlands: Springer. ISBN 978-1-4020-9597-9.

[7] Lessene G, Czabotar PE, 2008 Colman PM. BCL-2 family antagonists for cancer therapy. Nat Rev Drug Discov.;7:989-1000.

[8] R. J. Youle and A. Strasser, 2008 "The BCL-2 protein family: opposing activities that mediate cell death," Nature Reviews Molecular Cell Biology, vol. 9, no. 1, pp. 47–59.

[9] S. J. Korsmeyer, 1992 "Bcl-2: an antidote to programmed cell death," Cancer Surveys, vol. 15, pp. 105–118.
[10] Robert Eskes, Solange Desagher,Bruno Antonsson, andJean-Claude Martinou 2000 Bid Induces the Oligomerization and Insertion of Bax into the Outer Mitochondrial Membrane. Mol. Cell. Biol. February vol. 20 no. 3 929-935.
[11] Yuan CQ, Ding ZH. 2002 Structure and function of caspases.GuowaiYixueFenzi Shengwuxue Fence, 24: 146−151.
[12] Y. Tsujimoto, J. Gorham, and J. Cossman, 1985 "The t(14;18) chromosome translocations involved in B-cell neoplasms result from mistakes inVDJ joining," Science, vol. 229, no. 4720, pp. 1390–1393.